

Distributional Smoothing with Virtual Adversarial Training

Takeru Miyato

MIYATO-T@SYS.I.KYOTO-U.AC.JP

Shin-ichi Maeda

ICHI@SYS.I.KYOTO-U.AC.JP

Masanori Koyama

KOYAMA-M@SYS.I.KYOTO-U.AC.JP

Ken Nakae

NAKAE-K@SYS.I.KYOTO-U.AC.JP

Shin Ishii

ISHII@I.KYOTO-U.AC.JP

Graduate School of Informatics, Kyoto University, Yoshidahonmachi 36-1, Sakyo, Kyoto, Japan

Abstract

Smoothness regularization is a popular method to decrease generalization error. We propose a novel regularization technique that rewards local distributional smoothness (LDS), a KL-distance based measure of the model’s robustness against perturbation. The LDS is defined in terms of the direction to which the model distribution is most sensitive in the input space. We call the training with LDS regularization the virtual adversarial training (VAT). Our technique resembles the adversarial training (Goodfellow et al., 2015), but distinguishes itself in that it determines the adversarial direction from the model distribution alone, and does not use the label information. The technique is therefore applicable even to semi-supervised learning. When we applied our technique to the classification task of the permutation invariant MNIST dataset, it not only eclipsed all the models that are not dependent on generative models and pre-training, but also performed well even in comparison to the state of the art method (Rasmus et al., 2015) that uses a highly advanced generative model.

Keywords: adversarial training, deep neural network, regularization, supervised learning, semi-supervised learning

1. Introduction

Overfitting is an unavoidable challenge in supervised and semi-supervised training of the classification and regression functions. When the training samples is finite, the training error computed from the empirical distribution of the training samples is bound to be different from the test error, which is the expectation of the log-likelihood with respect to the true underlining probability measure. The asymptotic analysis (Akaike, 1998; Watanabe, 2009) is useful in determining the extent of the diversion of the training error from the test error. Unfortunately, asymptotic analysis like AIC can only describe the asymptotic behavior of the expectation. They are unable to completely resolve the indeterminacy of the true distribution.

The most major countermeasure against overfitting is the inclusion of the regularization function into the cost function that originally consists of the log-likelihood alone, which is highly dependent on the size of the dataset. The addition of the regularization term diminishes the relative dependence of the training process on the likelihood term. As a result, the model distribution that optimizes the regularized cost function is less affected by the size of the dataset. L_2 and L_1 regularizations are popular methods (Friedman et al.,

2001). However, except for the case of simple models like linear regression, the effects of the L_2 and L_1 regularization terms on the model distribution can be complex. This is especially true for the complex models like deep neural networks (Bengio, 2009; LeCun et al., 2015). Moreover, reparametrization alters the effects of the L_2 and L_1 regularizations on the model distribution, and hence the identity of the model distribution that optimizes cost function.

For the ultimate goal of decreasing the generalization error, regularization function that reflects our belief on the true distribution is ideal. In many familiar subjects like image and time-series analyses, a smooth model distribution tends to perform better than other non-smooth distributions (Wahba, 1990) in terms of the generalization error. Throughout this article, we therefore adopt this belief on the ‘good model’. We also seek the loss function $T(\theta)$ that is parameterization invariant. That is, if $\theta = \theta^*$ is the parameter that minimizes the cost function and if $\eta = f(\theta)$, the reparametrized cost function $\tilde{T}(\eta)$ should take the minimum value at $\eta = f(\theta^*)$.

Adversarial training (Goodfellow et al., 2015) is the newest brand of parameterization invariant smoothness regularization. It is a method that aims to improve the local smoothness of the model in the neighborhood of every observed data point. At each step of the training, Goodfellow et al. identified for each pair of the observed input and output the direction of the input perturbation to which the classifier’s label assignment is most sensitive. Goodfellow et al. then penalized the model’s sensitivity with respect to the perturbation in the adversarial direction.

We propose a novel parameterization invariant smoothness regularization that builds on the philosophy of the adversarial training. At each step in the training, we identify for each observed input the perturbation to which the model distribution itself is most sensitive in the sense of Kullback-Leibler divergence (KL divergence). This perturbation is determined without the label information of the observed input. At each input, we can therefore define the robustness of the model distribution against the perturbation in a local and ‘virtual’ adversarial direction. The local robustness defined this way serves as a measure of the local smoothness of the distribution, which we call the local distributional smoothness (LDS). We propose virtual adversarial training (VAT), a simple regularization technique that rewards the average of the LDS over all the training samples. Because the LDS is independent of the label informations, VAT is applicable to the semi-supervised learning.

When we applied the VAT to the semi-supervised and supervised learning for the permutation invariant MNIST task, our method not only outperformed all the models that are not dependent on generative models or pre-training, but it also performed well even in comparison to the state of the art method (Rasmus et al., 2015) that uses a highly advanced generative model.

2. Methods

2.1. Formalization of Local Distributional Smoothness

We begin with the formal definition of the local distributional smoothness. Let us suppose the input space \mathfrak{R}^I , the output space Q , and a training samples

$$D = \{(x^{(n)}, y^{(n)}) | x^{(n)} \in \mathfrak{R}^I, y^{(n)} \in Q, n = 1, \dots, N\},$$

and consider the problem of using D to train the model distribution $p(y|x, \theta)$ parametrized by θ . Let $\text{KL}[p||q]$ denote the KL divergence between the distributions p and q . Also, with the hyperparameter $\epsilon > 0$, we define

$$\Delta_{\text{KL}}(r, x^{(n)}, \theta) \equiv \text{KL}[p(y|x^{(n)}, \theta) || p(y|x^{(n)} + r, \theta)] \quad (1)$$

$$r_{\text{v-adv}} \equiv \arg \min_r \{-\Delta_{\text{KL}}(r, x^{(n)}, \theta); \|r\|_2 \leq \epsilon\}. \quad (2)$$

We define the LDS of the model distribution at $x^{(n)}$ by

$$\text{LDS}(x^{(n)}, \theta) \equiv -\Delta_{\text{KL}}(r_{\text{v-adv}}, x^{(n)}, \theta). \quad (3)$$

From now on, we refer to $r_{\text{v-adv}}$ as the virtual adversarial perturbation. Note $r_{\text{v-adv}}$ is the direction to which the model distribution $p(y|x^{(n)}, \theta)$ is most sensitive in the sense of KL divergence. In a way, this is a KL divergence analogue of the gradient ∇_x of the model distribution with respect to the input, and perturbation of x in this direction wrecks the local smoothness of $p(y|x^{(n)}, \theta)$ at $x^{(n)}$ in a most dire way. The smaller the value of $\Delta_{\text{KL}}(r_{\text{v-adv}}, x^{(n)}, \theta)$ at $x^{(n)}$, the smoother the $p(y|x^{(n)}, \theta)$ at x . Our goal is to improve the smoothness of the model in the neighborhood of all the observed inputs. Formulating this goal based on the LDS, we obtain the following objective function,

$$\sum_{n=1}^N \log p(y^{(n)}|x^{(n)}, \theta) + \lambda \sum_{n=1}^N \text{LDS}(x^{(n)}, \theta), \quad (4)$$

We call the training based on (4) the virtual adversarial training (VAT). By the construction, VAT is parametrized by the hyperparameter $\lambda > 0$ and $\epsilon > 0$. If we define $r_{\text{adv}} \equiv \arg \min_r \{p(y^{(n)}|x^{(n)} + r, \theta), \|r\|_p \leq \epsilon\}$ and replace $\Delta_{\text{KL}}(r, x^{(n)}, \theta)$ in (3) with $\Delta_{\text{margin}}(r_{\text{adv}}, x^{(n)}, \theta) = \log p(y^{(n)}|x^{(n)} + r_{\text{adv}}, \theta)$, we obtain the objective function of the adversarial training. Perturbation of $x^{(n)}$ in the direction of $r_{\text{adv}}(x^{(n)})$ can most severely damage the probability that the model correctly assigns the label $y^{(n)}$ to $x^{(n)}$. As opposed to r_{adv} , the definition of $r_{\text{v-adv}}$ on $x^{(n)}$ does not require the correct label $y^{(n)}$. This property allows us to apply the VAT to semi-supervised learning.

The LDS is a general notion that can be applied to any machine learner. For example, let us consider the linear regression model $p(y|x, \theta) = \mathcal{N}(\theta^T x, \sigma^2)$. Then, because the entropy of the Gaussian distribution does not depend on its mean, straightforward computation yields

$$\begin{aligned} \text{LDS}(x^{(n)}, \theta) &= \max_{\{r; \|r\|_2 \leq \epsilon\}} \text{KL}[p(y|x^{(n)}, \theta) || p(y|x^{(n)} + r, \theta)] \\ &= -H(p(y|x^{(n)}, \theta)) + \max_{\{r; \|r\|_2 \leq \epsilon\}} \int p(y|x^{(n)}, \theta) \log p(y|x^{(n)} + r, \theta) dy \\ &\propto \max_{\{r; \|r\|_2 \leq \epsilon\}} (\theta^T r)^2 + \text{const} \\ &= \epsilon^2 \|\theta\|_2^2 + \text{const}, \end{aligned}$$

so that we obtain the same cost function as the L_2 regularization. We would emphasize, however, that this does not mean that the VAT is equivalent to the L_2 regularization on the linear regression model. Let θ^3 denote the component-wise third order exponentiation. It is not difficult to see that, when we reparametrize the model as $p(y|x, \theta) = \mathcal{N}(\theta^{3T} x, \sigma^2)$, we obtain $\text{LDS}(x^{(n)}, \theta^3) = \epsilon^2 \|\theta^3\|_2^2$, not $\epsilon^2 \|\theta\|_2^2$.

2.2. Efficient evaluation of LDS and its derivative with respect to θ

Once $r_{\text{v-adv}}$ is computed, the evaluation of the LDS is simply the computation of the KL divergence between the model distributions $p(y|x^{(n)}, \theta)$ and $p(y|x^{(n)} + r_{\text{v-adv}}, \theta)$, which is relatively straightforward. In what follows, we discuss the efficient computation of $r_{\text{v-adv}}$, for which there is no evident approximation.

2.2.1. EVALUATION OF $r_{\text{v-adv}}$

We assume that $p(y|x, \theta)$ is differentiable with respect to θ and x almost everywhere. Because $\Delta_{\text{KL}}(r, x, \theta)$ takes minimum value at $r = 0$, the differentiability assumption dictates that its first derivative $\nabla_r \Delta_{\text{KL}}(r, x, \theta)|_{r=0}$ is zero. Therefore we can take the second-order Taylor approximation as

$$\Delta_{\text{KL}}(r, x, \theta) \cong r^T H_r(x, \theta) r, \quad (5)$$

where $H_r(x, \theta)$ is a Hessian matrix given by $H_r(x, \theta) \equiv \nabla \nabla_r \Delta_{\text{KL}}(r, x, \theta)|_{r=0}$. Under this approximation $r_{\text{v-adv}}$ emerges as the first dominant eigenvector of $H_r(x, \theta)$, $u(x, \theta)$, of magnitude ϵ ,

$$\begin{aligned} r_{\text{v-adv}}(x, \theta) &\cong \arg \min_r \{r^T H_r(x, \theta) r, \|r\|_2 \leq \epsilon\} \\ &= \overline{\epsilon u(x, \theta)}, \end{aligned} \quad (6)$$

where $\bar{\cdot}$ denotes an operator acting on arbitrary non-zero vector v that returns a unit vector in the direction of v as \bar{v} . Hereafter, we denote $H_r(x, \theta)$, $r_{\text{v-adv}}(x, \theta)$ and $u(x, \theta)$ as H_r , $r_{\text{v-adv}}$ and u , respectively. As depicted in Figure 1, the approximated $r_{\text{v-adv}}$ is the direction of the shortest axis of the ellipse representing the contour of $\Delta_{\text{KL}}(r, x, \theta)$.

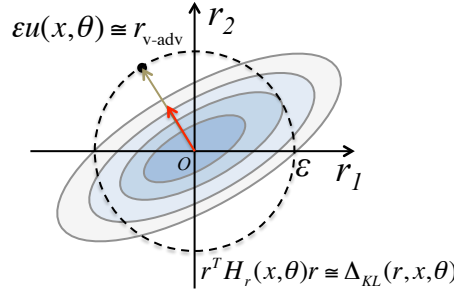


Figure 1: Contour of $\Delta_{\text{KL}}(r, x, \theta)$ and the direction $r_{\text{v-adv}}$

The eigenvector of the Hessian $H_r(x, \theta)$ and its eigenvectors require $O(I^3)$ computational time, which becomes unfeasibly large for high dimensional input space. We therefore resort to power iteration method and finite difference method to approximate $r_{\text{v-adv}}$. Let d be a randomly sampled unit vector. As long as d is not perpendicular to the dominant eigenvector u , the iterative calculation of

$$d \leftarrow \overline{H_r d} \quad (7)$$

will make the d converge to u . We need to do this without the direct computation of H_r , however. $H_r d$ can be approximated by finite difference:

$$\begin{aligned} H_r d &\cong \frac{\nabla_r \Delta_{KL}(r + \xi d, x, \theta)|_{r=0} - \nabla_r \Delta_{KL}(r, x, \theta)|_{r=0}}{\xi} \\ &= \frac{\nabla_r \Delta_{KL}(r + \xi d, x, \theta)|_{r=0}}{\xi}, \end{aligned} \quad (8)$$

with $\xi \neq 0$. In the computation above, we used the fact $\nabla_r \Delta_{KL}(r, x, \theta)|_{r=0} = 0$ again. In summary, we can approximate $r_{\text{v-adv}}$ with the repeated application of the following update:

$$d \leftarrow \overline{\nabla_r \Delta_{KL}(r + \xi d, x, \theta)|_{r=0}}. \quad (9)$$

The approximation improves monotonically with the iteration times of the power method, I_p . Most notably, the value $\nabla_r \Delta_{KL}(r + \xi d, x, \theta)|_{r=0}$ can be computed easily by the back propagation method in the case of neural networks. We denote the approximated $r_{\text{v-adv}}$ as $\tilde{r}_{\text{v-adv}} = \text{GenVAP}(\theta, x^{(n)}, \epsilon, I_p, \xi)$ (See Algorithm 1), and denote the LDS computed with $\tilde{r}_{\text{v-adv}}$ as

$$\widetilde{\text{LDS}}(x^{(n)}, \theta) \equiv -\Delta_{KL}(\tilde{r}_{\text{v-adv}}, x^{(n)}, \theta). \quad (10)$$

Algorithm 1 Generation of $\tilde{r}_{\text{v-adv}}$

Function GenVAP($\theta, x^{(n)}, \epsilon, I_p, \xi$)

1. Initialize $d \in R^I$ by a random unit vector.
2. **Repeat For** i in $1 \dots I_p$ (Perform I_p -times power method)

$$d \leftarrow \overline{\nabla_r \Delta_{KL}(r + \xi d, x^{(n)}, \theta)|_{r=0}}$$

3. **Return** ϵd

2.2.2. EVALUATION OF DERIVATIVE OF APPROXIMATE LDS W.R.T θ

Now it remains to evaluate the derivative of $\widetilde{\text{LDS}}(x^{(n)}, \theta)$ with respect to θ . By definition, $\tilde{r}_{\text{v-adv}}$ depends on θ . Our numerical experiments, however, indicates that $\nabla_\theta r_{\text{v-adv}}$ is quite volatile with respect to θ , and we could not make effective regularization when we used the numerical evaluation of $\nabla_\theta r_{\text{v-adv}}$ in $\nabla_\theta \widetilde{\text{LDS}}(x^{(n)}, \theta)$. We have therefore followed the work of [Goodfellow et al. \(2015\)](#) and ignored the derivative of $\nabla_\theta \widetilde{\text{LDS}}(x^{(n)}, \theta)$ with respect to $\tilde{r}_{\text{v-adv}}(x^{(n)}, \theta)$

The stochastic gradient descent based on Eq. (4) with this derivative was able to successfully decrease the average $\widetilde{\text{LDS}}(x^{(n)}, \theta)$, and achieved good results in terms of generalization error. Interestingly, When we replaced

$$\frac{\partial}{\partial \theta} \widetilde{\text{LDS}}(x^{(n)}, \theta) \Big|_{\theta=\hat{\theta}}$$

with the approximation

$$-\frac{\partial}{\partial \theta} \text{KL}[p(y|x^{(n)}, \hat{\theta}) \| p(y|x^{(n)} + \tilde{r}_{\text{v-adv}}(x^{(n)}, \hat{\theta}), \theta)] \Big|_{\theta=\hat{\theta}} \quad (11)$$

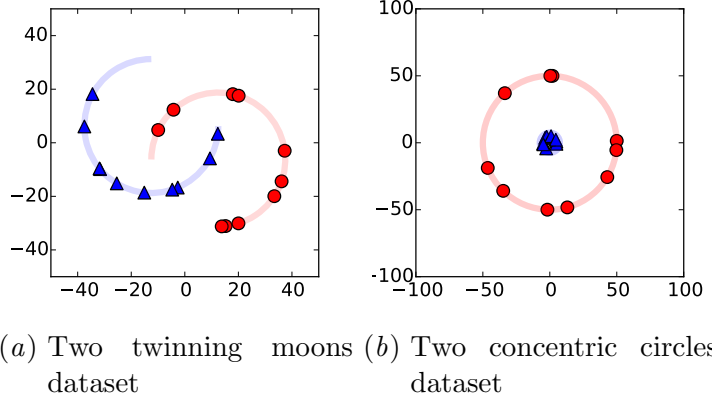


Figure 2: Visualization of the synthetic datasets. Each panel depicts the total of 20 training data points. Blue triangles stand for the samples with label 0 and the red circles stand for the samples with label 1. Samples with each label are prepared uniformly from the light-colored trajectory.

we were able to further decrease the average value of $\widetilde{\text{LDS}}(x^{(n)}, \theta)$ and improve the generalization performance. From now on, we refer to the training of the regularized likelihood (4) based on Eq. (11) as the virtual adversarial training (VAT).

3. Experiments

To evaluate the efficacy of VAT, we conducted two sets of experiments. Firstly, We applied various regularization techniques including VAT to the binary classification of synthetic datasets and visualized their effects on the classification boundaries. Secondly, we applied VAT to both the supervised and semi-supervised learning for the classification of MNIST dataset, and assessed its performance relative to the other regularization methods.

All the computations were conducted with Theano (Bergstra et al., 2010; Bastien et al., 2012) on a GPU environment. Reproducing code is under preparation.

3.1. Supervised learning for the binary classification of synthetic dataset

We created two synthetic datasets by generating multiple points uniformly over two trajectories on \mathbb{R}^2 as shown in Figure 2 and linearly embedding them into 500 dimensional vector space. The datasets are called (a) two twinning moons dataset (in short, ‘Moons’) and (b) two concentric circles dataset (in short, ‘Circles’) based on the shapes of the two trajectories, respectively. Each dataset consists of 20 training samples, 100 validation samples, and 1000 test samples. Validation sets were used to tune the hyper parameter ϵ . Because the number of the samples is very small relative to the input dimension, maximum likelihood estimation (MLE) is vulnerable to overfitting problem on this dataset. The set of hyper-parameters in each regularization method and the other detailed experimental settings are described in Appendix A.1. We repeated the experiments 50 times with different samples of training, validation and test sets, and reported the average of the 50 test performances.

Our classifier was a neural network (NN) with one hidden layer consisting of 500 hidden units. We used ReLU (Jarrett et al., 2009) activation function for hidden units, and used softmax activation function for all the output units. The regularization methods we compared against the VAT on this dataset include L_2 regularization ($L_2\text{-reg}$), dropout, adversarial training, and random perturbation training. The random perturbation training is a modified version of the VAT in which we replaced $r_{\text{v-adv}}$ with an ϵ sized unit vector uniformly sampled from I dimensional unit sphere. We compared random perturbation training with VAT in order to highlight the importance of choosing the appropriate direction of the perturbation. As for the adversarial training, we followed Goodfellow et al. (2015) and determined the size of the perturbation r in terms of both L_∞ (max) norm and L_2 norm.

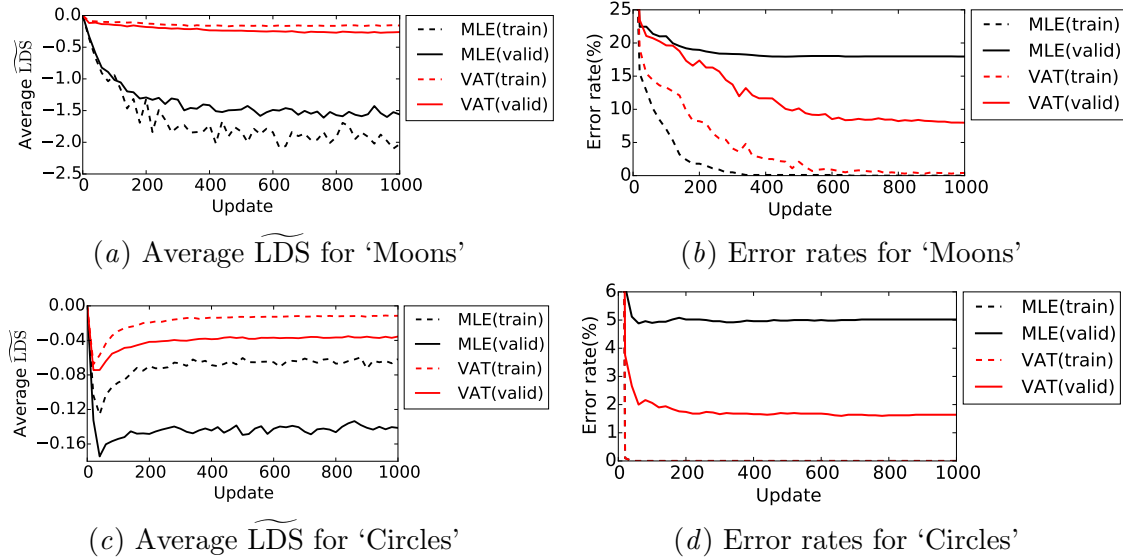


Figure 3: Comparison of learning curve between the MLE and the VAT implemented with $\epsilon' = 0.5$ and $I_p = 1$. Average $\widetilde{\text{LDS}}$ showed in (a) and (c) were evaluated on the training and validation samples with $\epsilon' = 0.5$ and $I_p = 10$. As for the detailed definition of ϵ' , we refer the reader to the Appendix A.1.

Figure 3 compares the learning process between the VAT and the MLE. Panels (a) and (c) show the learning curves of the average $\widetilde{\text{LDS}}$ while panels (b) and (d) show the learning curves of the error rate, on both validation set and training set. The average $\widetilde{\text{LDS}}$ is nearly zero at the beginning, because the models are initially close to uniform distribution. The average $\widetilde{\text{LDS}}$ then decreases slowly for the VAT, and falls rapidly for the MLE. Although the training error eventually drops to zero for both methods, the final validation error of the VAT is significantly lower than that of the MLE. This difference suggests that a high sustained value of $\widetilde{\text{LDS}}$ is beneficial in alleviating the overfitting and in decreasing the generalization error. Note that it is impossible to cover this difference with early stopping, because the minimum value of the validation error is significantly higher for the MLE than that for the VAT.

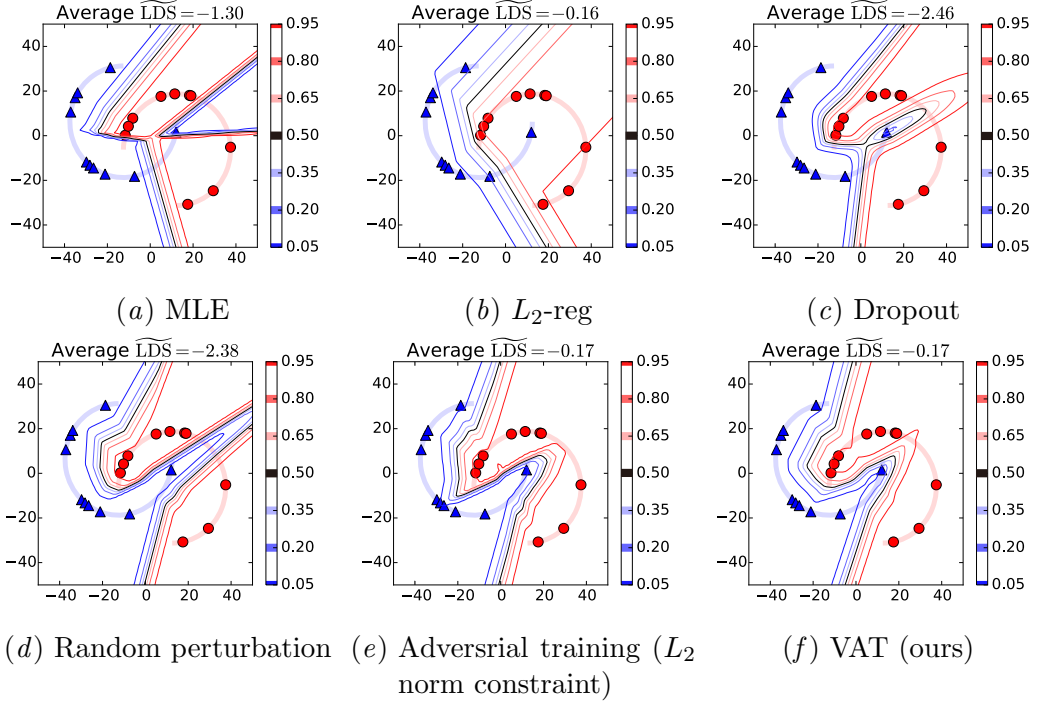


Figure 4: Contours of $p(y = 1|x, \theta)$ drawn by NNs (with ReLU activation) trained with various regularization methods for a single dataset of ‘Moons’. A black line represents the contour of value 0.5. Red circles represent the data points with label 1, and blue triangles represent the data points with label 0. Average $\widetilde{\text{LDS}}$ evaluated on the training set with $\epsilon' = 0.5$ and $I_p = 10$ is shown at the top of each panel. As for the detailed definition of ϵ' , we refer the reader to the Appendix A.1.

Figures 4 and 5 show the contour plot of model distributions trained by each method for ‘Moons’ and ‘Circles’¹, along with the corresponding average $\widetilde{\text{LDS}}$ values.

As we can see in Figure 4, only the adversarial training and VAT could obtain legitimate decision boundaries. In the set of regularization methods we tested in this comparative study, these two methods are the only methods that impose local constraints on the input-output relationship. Their average $\widetilde{\text{LDS}}$ s are high (-0.17 for both) compared to that of the MLE (-1.30). The preference to a high value of $\widetilde{\text{LDS}}$ is equivalent to the preference to less volatile model distribution and the decision boundary with larger margins. One can achieve very high value of $\widetilde{\text{LDS}}$ with the L_2 regularization as well, but only with the sacrifice of classification accuracy. By its definition, L_2 regularization cannot control the local smoothness. With the regularization term that does not depend on the input, L_2 regularization can only control global smoothness. Dropout was not effective in maintaining high $\widetilde{\text{LDS}}$ as well. Recall that dropout is a method to train an underlying ensemble of various model

1. Each panel shows the projection of the trained 500 dimensional model distribution onto the 2-dimensional space. The trained model distributions are based on the best hyperparameters and the ReLU activation function.

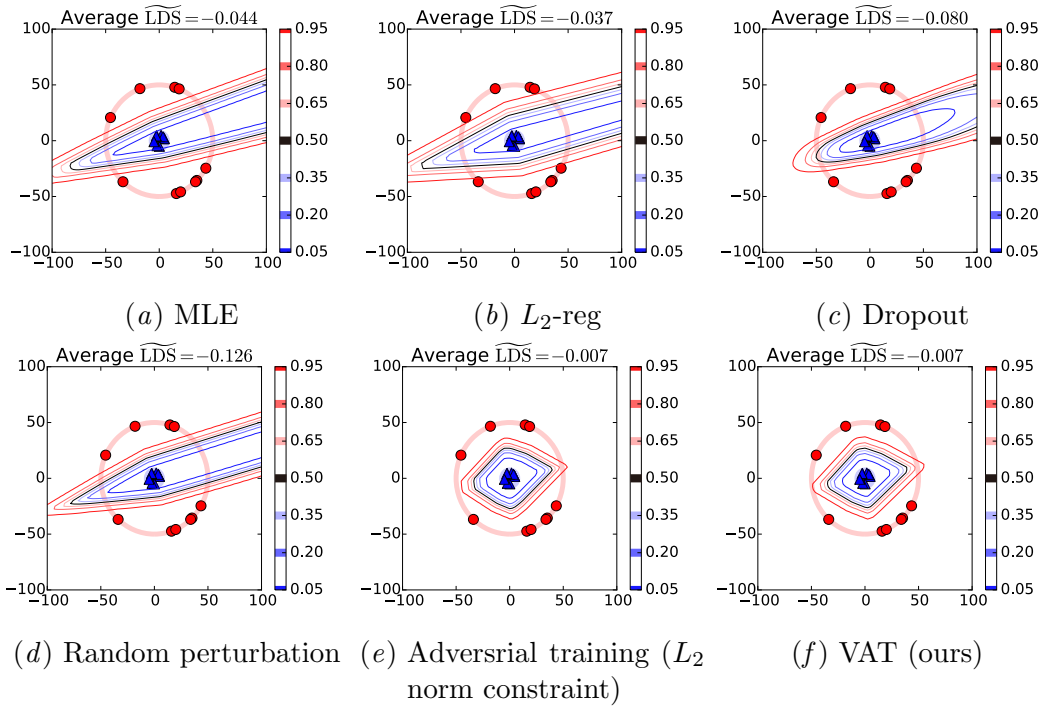


Figure 5: Contours of $p(y = 1|x, \theta)$ drawn by NNs (with ReLU activation) trained with various regularization methods for a single dataset of ‘Circles’.

structures. As pointed out in (Goodfellow et al., 2015; Szegedy et al., 2014), an adversarial example is also likely to cover wide range of model structures. The relatively low $\widetilde{\text{LDS}}$ value by dropout suggests that ‘ensemble’ training is not sufficient for making the models robust against adversarial examples. The random perturbation training showed even lower $\widetilde{\text{LDS}}$ value than that of the MLE. This indicates that one cannot avoid overfitting by blindly smoothing the model distribution around the observed data points, and that it is important to detect the direction in which the current model is least smooth at every step of the training.

Figure 5 shows similar results for ‘Circles’. Only the adversarial training and VAT could obtain legitimate decision boundaries, and the average $\widetilde{\text{LDS}}$ of these two methods was the lowest (both -0.007) among these six regularization methods. The random perturbation training again failed and exhibited a low value of $\widetilde{\text{LDS}}$.

Figure 6 shows the average test errors obtained by the NNs trained with the best set of hyperparameters and the ReLU activation function. The adversarial learning and VAT achieved much lower test errors than the other regularization methods. Surprisingly, the performance of the VAT did not change much with the value of I_p . ($I_p = 1, 4$). We therefore experimented with $I_p = 1$ for all sets of experiments on the MNIST dataset.

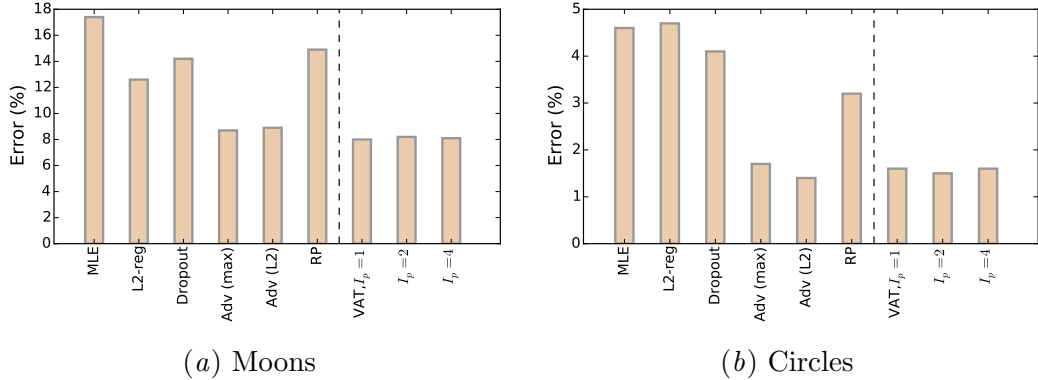


Figure 6: Comparison of the test error for (a) ‘Moons’ and (b) ‘Circles’ by NNs with the ReLU activation function. ‘RP’ indicates the random perturbation training method.

3.2. Supervised classification for the MNIST dataset

Next, we tested the performance of our regularization method on the MNIST dataset, which consists of 28×28 pixel images of handwritten digits and their corresponding labels. The input dimension is therefore $28 \times 28 = 784$ and each label is one of the numerals from 0 to 9. We split the original 60,000 training samples into 50,000 training samples and 10,000 validation samples, and used the latter of which to tune the hyperparameters. We applied our methods to the training of three types of NNs with different numbers of layers, 2, 3 and 4. As for the number of hidden units, we used (1200, 600), (1200, 600, 300), and (1200, 600, 300, 150), respectively. The ReLU activation function and batch normalization technique (Ioffe and Szegedy, 2015) were used for all the NNs. The detailed settings of the experiments are described in Appendix A.2.

For each regularization method, we used the set of hyperparameters that achieved the best performance on the validation data to train the NN on all training samples. We applied the trained networks to the test set and recorded their test errors. We repeated this procedure 20 times with different seeds for the weight initialization, and reported the average test error values.

Table 1 summarizes the test error obtained by our regularization method (VAT) and the other regularization methods. The test error of our VAT (0.644%) was comparable to that of the state of the art method (i.e., Ladder network, 0.61%). The VAT was also better than all of the other methods that are not dependent on generative models or pre-training.

3.3. Semi-supervised learning for classification of the MNIST dataset

Recall that our definition of LDS (Eq. (3)) at any point x is independent of the label information y . This in particular means that we can apply the VAT to semi-supervised learning tasks. We would like to emphasize that this is a property not enjoyed by adversarial example and dropout. We experimented with four sizes of labeled training samples $N_1 =$

Table 1: Test errors of 10-class supervised learning for the permutation invariant MNIST task. Stars * indicate the methods that are dependent on generative models or pre-training. Test errors in the upper panel are the ones reported in the literature, and test errors in the bottom panel are the outputs of our implementation.

Method	Test error (%)
Gaussian dropout (Srivastava et al., 2014)	0.95
Maxout Networks Goodfellow et al. (2013)	0.94
MTC* (Rifai et al., 2011)	0.81
DBM* (Srivastava et al., 2014)	0.79
Adversarial training(max norm) (Goodfellow et al., 2015)	0.782
Ladder network* (Rasmus et al., 2015)	0.61±0.05
Baseline	1.15
Random perturbation training	0.980
Adversarial training (max norm)	0.762
Adversarial training (L_2 norm)	0.713
VAT (ours)	0.644±0.027

$\{100, 600, 1000, 3000\}$ and observed the effect of N_l on the test error. We used the validation set of fixed size 1000, and used all the training samples excluding the validation set and the labeled to train the NNs. That is, when $N_1 = 100$, the unlabeled training set had the size of $60,000 - 100 - 1,000 = 58,900$. For each choice of the hyperparameters, we repeated the experiment 20 times with different set of $N_1 = 100$ sized labeled training data, and repeated the experiment 10 times with different set of $N_1 = \{600, 1000, 3000\}$ sized labeled training data. As for the architecture of NNs, we used ReLU based NNs with two hidden layers with the number of hidden units (1200, 1200). Batch normalization was implemented (Ioffe and Szegedy, 2015) as well. For more details, we refer the readers to Appendix A.3.

Table 2 summarizes the results. The VAT outperformed the methods like EmbedNN (Weston et al., 2012) and pseudo ensembles agreement (PEA) (Bachman et al., 2014) that are not dependent on generative models or pre-training. It was however not able to perform better than the Ladder network (Rasmus et al., 2015), the very recent state of the art method.

4. Discussion and Related Works

Our experiments based on the synthetic datasets and the MNIST dataset indicate that the VAT is an effective method for both supervised and semi-supervised learning. VAT outperformed all regularization methods that are not dependent on generative models or pre-training in the MNIST dataset. We would also like to emphasize the simplicity of the method. Models that relies heavily on generative models are dependent on many hyperparameters. VAT, on the other hand, has only two hyperparameters, ϵ and λ .

Our VAT was motivated by the adversarial training (Goodfellow et al., 2015). Adversarial training and VAT are similar in that they both use the local input-output relationship to smooth the model distribution in the corresponding neighborhood. In contrast, L_2 reg-

Table 2: Test errors of 10-class semi-supervised learning for the permutation invariant MNIST task. All values are the averages over random partitioning of the dataset. Stars * indicate the methods that are dependent on generative models or pre-training.

Method	N_l	Test error(%)			
		100	600	1,000	3,000
NN (Weston et al., 2012)		25.8	11.4	10.7	6.04
EmbedNN (Weston et al., 2012)		16.9	5.97	5.73	3.59
MTC* (Rifai et al., 2011)		12.0	5.13	3.64	2.57
PEA (Bachman et al., 2014)		10.79	2.44	2.23	1.91
PEA* (Bachman et al., 2014)		5.21	2.87	2.64	2.3
DG* (Kingma et al., 2014)		3.33	2.59	2.4	2.18
Ladder network* (Rasmus et al., 2015)		1.13		1.00	
VAT (ours)		2.12	1.40	1.32	1.24

ularization does not use the local input-output relationship, and cannot introduce local smoothness to the model distribution. Increasing of the regularization constant in L_2 regularization can only intensify the global smoothing of the distribution, which results in lower generalization error.

The adversarial training aims to train the model while keeping the average of the following value high:

$$\min_r \{ \log p(y^{(n)}|x^{(n)} + r, \theta), \|r\|_p \leq \epsilon \}. \quad (12)$$

This makes the likelihood evaluated at the n -th labeled data point robust against ϵ -perturbation applied to the input in its adversarial direction.

PEA (Bachman et al., 2014), on the other hand, used the model's sensitivity to random perturbation on input and hidden layers in their construction of the regularization function. PEA is similar to the random perturbation training of our experiment in that it aims to make the model distribution robust against random perturbation. However, as shown in the failure of random perturbation training, the benefit of making the model robust against completely random perturbation is questionable. In fact, PEA was not able to outperform dropout (Srivastava et al., 2014) in supervised learning. VAT is decisively different from PEA in that VAT aims to make the model distribution robust against a very specific direction at each data point.

Deep contractive network by Gu and Rigazio (Gu and Rigazio, 2015) takes still another approach to smooth the model distribution. Gu et al introduced a penalty term based on the Frobenius norm of the Jacobian of $y = f(x, \theta)$ with respect to x . Instead of computing the computationally expensive full Jacobian, they approximated the Jacobian by the sum of the Frobenius norm of the Jacobian over every adjacent pairs of hidden layers. The deep contractive network was, however, unable to significantly decrease the test error.

Ladder network (Rasmus et al., 2015) is a method that uses layerwise denoising autoencoder. Their method is currently the best method in both supervised and semi-supervised

learning for permutation invariant MNIST task. Ladder network seems to be conducting a variation of manifold learning that extracts the knowledge of the local distribution of the inputs. VAT, on the other hand, uses the property of the conditional distribution $p(y|x, \theta)$ only, giving no consideration to the generative process $p(x|y, \theta)$ nor to the joint distribution $p(y, x|\theta)$. In this aspect, VAT can be complementary to the methods that explicitly model the input distribution. We might be able to improve VAT further by introducing the notion of manifold learning into its framework.

References

Hirotugu Akaike. Information theory and an extension of the maximum likelihood principle. In *Selected Papers of Hirotugu Akaike*, pages 199–213. Springer, 1998.

Phil Bachman, Ouais Alsharif, and Doina Precup. Learning with pseudo-ensembles. In *Advances in Neural Information Processing Systems*, 2014.

Frédéric Bastien, Pascal Lamblin, Razvan Pascanu, James Bergstra, Ian J. Goodfellow, Arnaud Bergeron, Nicolas Bouchard, and Yoshua Bengio. Theano: new features and speed improvements. Deep Learning and Unsupervised Feature Learning NIPS 2012 Workshop, 2012.

Yoshua Bengio. Learning deep architectures for ai. *Foundations and trends® in Machine Learning*, 2(1):1–127, 2009.

James Bergstra, Olivier Breuleux, Frédéric Bastien, Pascal Lamblin, Razvan Pascanu, Guillaume Desjardins, Joseph Turian, David Warde-Farley, and Yoshua Bengio. Theano: a CPU and GPU math expression compiler. In *Proceedings of the Python for Scientific Computing Conference (SciPy)*, June 2010. Oral Presentation.

Jerome Friedman, Trevor Hastie, and Robert Tibshirani. The elements of statistical learning. *Springer series in statistics Springer, Berlin*, 2001.

Ian J Goodfellow, David Warde-Farley, Mehdi Mirza, Aaron Courville, and Yoshua Bengio. Maxout networks. In *International Conference on Machine Learning*, 2013.

Ian J Goodfellow, Jonathon Shlens, and Christian Szegedy. Explaining and harnessing adversarial examples. In *International Conference on Learning Representation*, 2015.

Shixiang Gu and Luca Rigazio. Towards deep neural network architectures robust to adversarial examples. In *International Conference on Learning Representation*, 2015.

Sergey Ioffe and Christian Szegedy. Batch normalization: Accelerating deep network training by reducing internal covariate shift. In *International Conference on Machine Learning*, 2015.

Kevin Jarrett, Koray Kavukcuoglu, Marc’Aurelio Ranzato, and Yann LeCun. What is the best multi-stage architecture for object recognition? In *Computer Vision, 2009 IEEE 12th International Conference on*, pages 2146–2153. IEEE, 2009.

Diederik Kingma and Jimmy Ba. Adam: A method for stochastic optimization. In *International Conference on Learning Representation*, 2015.

Diederik Kingma, Shakir Mohamed, Danilo Jimenez Rezende, and Max Welling. Semi-supervised learning with deep generative models. In *Advances in Neural Information Processing Systems*, 2014.

Yann LeCun, Yoshua Bengio, and Geoffrey Hinton. Deep learning. *Nature*, 521(7553):436–444, 2015.

Antti Rasmus, Harri Valpola, Mikko Honkala, Mathias Berglund, and Tapani Raiko. Semi-supervised learning with ladder network. *arXiv preprint arXiv:1507.02672*, 2015.

Salah Rifai, Yann N Dauphin, Pascal Vincent, Yoshua Bengio, and Xavier Muller. The manifold tangent classifier. In *Advances in Neural Information Processing Systems*, 2011.

Nitish Srivastava, Geoffrey Hinton, Alex Krizhevsky, Ilya Sutskever, and Ruslan Salakhutdinov. Dropout: A simple way to prevent neural networks from overfitting. *The Journal of Machine Learning Research*, 15(1):1929–1958, 2014.

Christian Szegedy, Wojciech Zaremba, Ilya Sutskever, Joan Bruna, Dumitru Erhan, Ian Goodfellow, and Rob Fergus. Intriguing properties of neural networks. In *International Conference on Learning Representation*, 2014.

Grace Wahba. Spline models for observational data. *Siam*, 1990.

Sumio Watanabe. Algebraic geometry and statistical learning theory. *Cambridge University Press*, 2009.

Jason Weston, Frédéric Ratle, Hossein Mobahi, and Ronan Collobert. Deep learning via semi-supervised embedding. In *Neural Networks: Tricks of the Trade*, pages 639–655. Springer, 2012.

Appendix A. Details of experimental settings

A.1. Supervised binary classification for synthetic datasets

In this section, we provide the details of the parameter initialization for NNs we trained for synthetic datasets. Weight parameters between input and hidden layers were initialized with $N(0, 0.001^2)$, and those between hidden and output layers were all initialized at 0. Initial bias parameters were all set at 0. In the adversarial training, the search range of the hyperparameter ϵ depends on the choice of the norm; for example, a vector v with $\|v\|_\infty \leq \epsilon$ can take as large $\|v\|_2$ norm as $\epsilon\sqrt{I}$, where I is the input dimension. To reduce such an effect, we defined $\epsilon = \epsilon'\sqrt{I}$, and used ϵ' in place of ϵ in setting the parameter range of L_2 .

We list the search space for the hyperparameters below:

- L_2 regularization (L_2 -reg):
balance parameter $\lambda = \{0.0001, 0.0002, 0.0005, 0.001, \dots, 0.5, 1.0, 2.0, 5.0, 10.0\}$

- Dropout:
dropout rate (common for both hidden and input layers) $p(z) = \{0.1, 0.2, \dots, 0.9\}$
- Adversarial training (Max norm): $\epsilon = \{0.05, 0.1, 0.2, 0.5, 1.0, 2.0, 5.0\}$, $\lambda = 1$
- Adversarial training (L_2 norm): $\epsilon' = \{0.05, 0.1, 0.2, 0.5, 1.0, 2.0, 5.0\}$, $\lambda = 1$
- Random perturbation training: $\epsilon' = \{0.05, 0.1, 0.2, 0.5, 1.0, 2.0, 5.0\}$, $\lambda = 1$
- Virtual adversarial training: $\epsilon' = \{0.05, 0.1, 0.2, 0.5, 1.0, 2.0, 5.0\}$, $\lambda = 1$

As for the training we used stochastic gradient descent (SGD) with a moment method. When $J(\theta)$ is the objective function, the moment method augments the simple update in the SGD with a term dependent on the previous update $\Delta\theta_{i-1}$:

$$\Delta\theta_i = \mu_i \Delta\theta_{i-1} + (1 - \mu_i) \gamma_i \frac{\partial}{\partial \theta} J(\theta). \quad (13)$$

In the expression above, $\mu_i \in [0, 1]$ stands for the strength of the momentum, and γ_i stands for the learning rate. In our experiment, we used $\mu_i = 0.9$, and exponentially decreasing γ_i with rate 0.995. As for the choice of γ_1 , we used either 0.5 or 1.0. We trained the NNs with 1,000 parameter updates.

A.2. Supervised classification for the MNIST dataset

We provide more details of experimental settings on supervised classification for the MNIST dataset. Weight parameters in the NN's output layer were initialized at 0, and the rests were initialized randomly with $N(0, 0.001^2)$. Bias parameters were all initialized with 0. Following lists summarizes the ranges from which we searched for the best hyperparameters of each regularization method:

- Adversarial training (max norm): $\epsilon = \{0.025, 0.05, 0.075, 0.1\}$, $\lambda = 1$
- Adversarial training (L_2 norm): $\epsilon' = \{0.025, 0.05, 0.075, 0.1\}$, $\lambda = 1$
- Random perturbation training: $\epsilon' = \{0.25, 0.5, 0.75, 1.0\}$, $\lambda = 1$
- Virtual Adversarial training: $\epsilon' = \{0.025, 0.05, 0.075, 0.1\}$, $\lambda = 1$

The training was conducted by mini-batch SGD based on ADAM (Kingma and Ba, 2015). We chose the mini-batch size of 100, and used the default values of Kingma and Ba (2015) for the tunable parameters of ADAM. We trained the NNs with 50,000 parameter updates. As for the base learning rate in validation, we selected the initial value of 0.002 and adopted the schedule of exponential reduction with rate 0.9 per 500 updates. After the hyperparameter determination, we trained the NNs over 60,000 parameter updates. For the learning coefficient, we used the initial value of 0.002 and adopted the schedule of exponential reduction with rate 0.9 per 600 updates.

A.3. Semi-supervised classification for the MNIST dataset

We provide more details of experimental settings on semi-supervised classification for the MNIST dataset. Weights were initialized in the same way as in the supervised classification for MNIST. We searched for the best hyperparameter ϵ' from $\{0.0075, 0.01, 0.0125, 0.015, 0.0175\}$ in the $N_l = 100$ case. Best ϵ' was selected from $\{0.025, 0.05, 0.075, 0.1\}$ for all other cases.

All experiments were conducted with $\lambda = 1$ and $I_p = 1$.

For the optimization method, we again used ADAM-based minibatch SGD with the same hyperparameter values as those in the supervised setting. We note that, in the computation of ADAM, the likelihood term can be computed from labeled data only. We therefore used two separate minibatches at each step: one minibatch of size 100 from labeled samples for the computation of the likelihood term, and another minibatch of size 250 from both labeled and unlabeled samples for computing the regularization term. We trained the NNs over 50,000 parameter updates. For the learning rate, we used the initial value of 0.002 and adopted the schedule of exponential reduction with rate 0.9 per 500 updates.